



OPEN

Drought characteristics and its elevation dependence in the Qinghai–Tibet plateau during the last half-century

Wei Feng^{1,2}, Hongwei Lu¹✉, Tianci Yao^{1,2} & Qing Yu^{1,2}

Associated with global warming, drought has destructive influences on agriculture and ecosystems, especially in the fragile Qinghai–Tibet Plateau (QTP). This study investigated spatial–temporal patterns of meteorological drought in the QTP and its surrounding areas and made an attempt to explore the relationship between drought conditions and elevation. Robust monitoring data from 274 meteorological stations during 1970–2017 were analyzed using the Sen’s slope method, Mann–Kendall trend test and rescaled range analysis. Results revealed that under the wetting trend in the QTP, Standardized Precipitation Evapotranspiration Index (SPEI) increased of maximum 0.012/year in spring. Moreover, severe drought frequency in winter and future drought risk in summer also showed an increasing trend. Wetter trends were positively correlated with elevation, with a key point being 4,000 m where the change trend above 4,000 m was about 6.3 times of that below 4,000 m in study area. The difference of drought severities between SPEI in the QTP and its surrounding areas has increased from –0.19 in 1970 to 0.38 in 2017 and kept growing in future.

Drought is one of the most widespread and costly natural disasters¹, which can endanger the production of agriculture and animal husbandry, worsen the ecological environment, and even expose human to the risk of disease^{2,3}. Previous studies have suggested that under global warming, the percentage of dry areas in the world has increased by approximately 1.74% per decade during 1950–2008^{4,5}. With an average elevation above 4,000 m and an area of 200,000 square kilometers, the Qinghai–Tibet Plateau (QTP) is the source of major rivers in Asia^{6–8}. It is extremely vulnerable to global change, and easily suffers from drought. The drought herein will have profound impacts on the neighboring regions. Therefore, a comprehensive understanding of drought characteristics in the QTP is of great importance.

Many studies on spatiotemporal characteristics of drought in the QTP and its surrounding areas have been conducted, mainly concluded that the QTP has become warmer and wetter in the past decades, especially in the vast northwestern QTP^{5,7,9–13}. Additionally, Gao et al.⁸ analyzed the aridity changes using P/PET ratio in recent 30 years based on 83 stations, and found that the eastern QTP was becoming drier and the aridity change pattern was significantly correlated with precipitation, sunshine duration and diurnal temperature range. Liang et al.¹⁴ investigated 74 stations in the QTP during 1980–2014 and found that the drought pattern exhibited obvious inter-decadal variation and severe drought mainly occurred before the 1990s. Yang et al.¹⁵ forecasted an increasing drought trend in southwest China (including Yunnan Province) but an increasing wetting trend for the QTP based on simulation of Global Climate Models (GCM) taken from the Coupled Model Intercomparison Project Phase 5 (CMIP5) framework. Other studies have addressed the seasonal drought evolution in the QTP. Some concluded that the drought mainly decreased in spring, and a slight drying trend could be traced in winter^{16,17}; in autumn, extreme drought frequency increased in the eastern QTP but decreased in the northern region. Wang et al.¹⁸ used the self-calibrating Palmer Drought Severity Index (scPDSI) to investigate the drought variation between 1961–2009 and revealed that the southern QTP experienced a significant wetting trend although the northern QTP became significantly drier, particularly in spring and autumn. Apparently, different opinions exist in seasonal drought variations in the QTP and further investigations are thus desired.

¹Key Laboratory of Water Cycle and Related Land Surface Processes, Institute of Geographic Sciences and Natural Resources Research, Chinese Academy of Sciences, Beijing 100101, China. ²University of Chinese Academy of Sciences, Beijing 100049, China. ✉email: luhw@igsrr.ac.cn

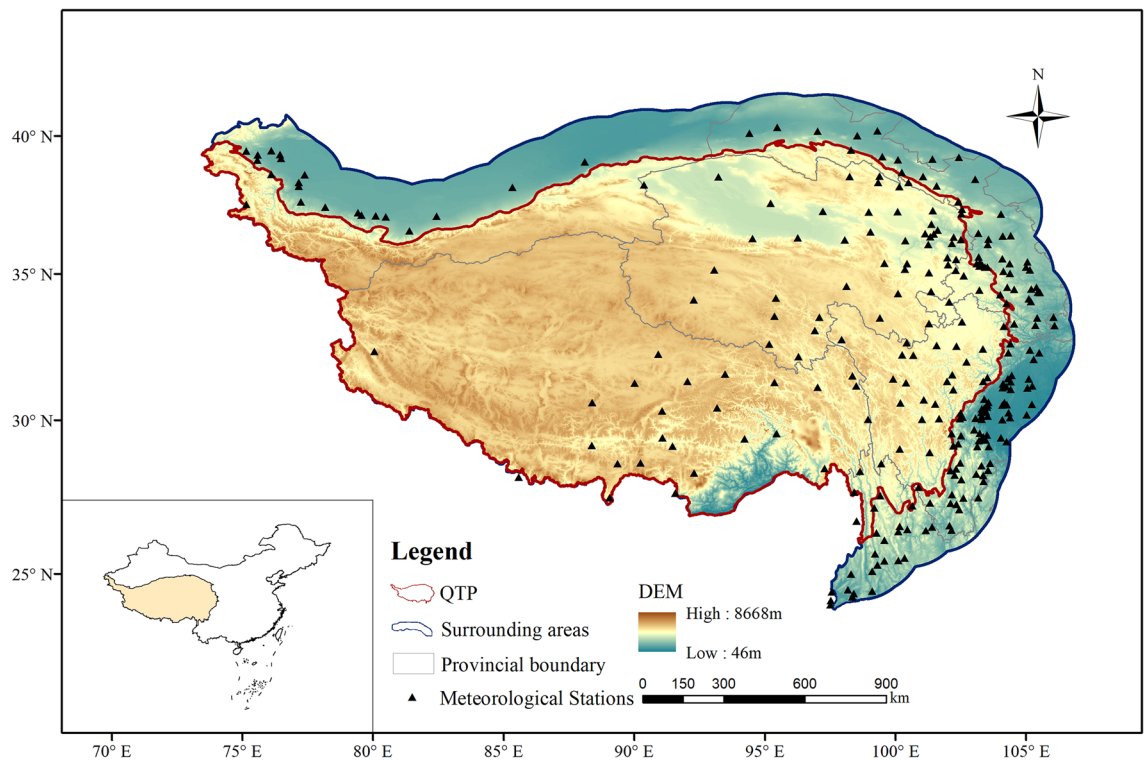


Figure 1. Study region and location of meteorological stations. The map was created using ArcMap 10.2, URL: <https://www.esrichina-bj.cn/softwareproduct/ArcGIS/>.

Understanding the climatic trends in highland regions is important and necessary for supporting global change studies because of their sensitivity and vulnerability to climate change¹⁹. Due to the drastic elevation changes, the QTP is a favorable place to explore the relationship between climate change and elevation. According to previous studies, mountainous areas are more sensitive to climate change compared to low-altitude areas at the same latitude^{20–22}. In recent years, many scientists have focused on elevation-related climate change researches, confirming the evidences of the elevation-dependent warming^{21,23}. Some have revealed that the warming trend displayed a slight decrease with elevation over 4,000 m²⁴, Zhang et al.²⁵ found smaller changes of PET in high-elevation areas at both annual and seasonal scales. Li et al.²⁶ concluded an increasing tendency of the precipitation with increasing elevation in summer. However, knowledge on elevation dependence of drying or wetting trends over the QTP is not well understood, particularly under low monitoring data availability and complex terrain conditions (low remote-sensing applicability).

Investigating drought trends in mountainous regions at different time scales along the elevation gradient is of great significance for thoroughly exploring drought phenomenon. In this study, monitoring data from 274 meteorological stations in the past 48 years were used to analyze wet and dry conditions evolutions over the QTP and its surrounding areas. The main objectives of this study were to: (1) assess the spatial distribution and temporal variation of drought, particularly severe drought in the QTP during 1970 to 2017; (2) explore how drought changes with elevation in the QTP and their possible causes; (3) discuss the persistence of drought trends.

Materials and methods

Study area and data. The study area locates in southwest China (24.0–40.3°N, 75.1–106.1°E) (Fig. 1). In order to explore the spatial–temporal pattern of drought in the QTP, particularly relationships between drought and elevation, a 200 km buffer zone based on the QTP boundary within the Chinese border was established by using the ArcGIS 10.2, namely “the surrounding areas”. The study area is thus composed of two parts, i.e. QTP and the surrounding areas. It includes Qinghai Province, Tibet Autonomous Region, part of Gansu Province, northern Yunnan Province, western Sichuan Province, part of Ningxia Hui Autonomous Region and southern Xinjiang Uygur Autonomous Region (Fig. 1). The average annual temperature of the study region reduced from 22 °C in the southeast to below –7 °C in the northwest. As the warm and humid air mass moving from the Indian Ocean is blocked by huge mountains, average annual precipitation has also reduced from 2,597 mm to less than 1.9 mm from southeast to northwest. The QTP is the origin of many rivers in Asia including the Yarlung Zangbo River, Nu River, Yangtze River, Yellow River and Lancang River. It also comprises a series of high mountains such as the Kunlun, Qilian, Tanggula and Hengduan mountains. Because of its special geographic location and large-scale topography, the QTP has a strong impact on both regional and global climates.

The meteorological data (i.e. daily precipitation and temperature) covering 274 stations (Fig. 1) during 1970–2017 were obtained from the Data Center for Resources and Environmental Science, Chinese Academy of Sciences (<https://www.resdc.cn/>). The dataset has been widely used in many studies^{27–30}. 115 of them locate in

Categories	SPEI values
No drought	$-0.5 < \text{SPEI}$
Mild drought	$-1.0 < \text{SPEI} \leq -0.5$
Moderate drought	$-1.5 < \text{SPEI} \leq -1.0$
Severe drought	$-2.0 < \text{SPEI} \leq -1.5$
Extreme drought	$\text{SPEI} \leq -2.0$

Table 1. Categories of drought grade based on SPEI¹.

the QTP and 159 of them are distributed in the buffer zone. The originally observed data were processed through standard quality control by the Data Center.

Methods. *Standardized precipitation evapotranspiration index.* SPEI as an improved drought index of SPI was first proposed by Vicente-Serrano et al.³¹. It has many advantages and was widely used in many studies^{17,32,33}. Compared to SPI, it adds temperature upon precipitation and can reveal the effects of global warming on drought³⁴. Potential evapotranspiration (PET) is a key part of the SPEI. Different methods have been proposed to estimate PET over the past decades. Some of them are based on physical mechanism, such as the FAO-56 Penman–Monteith method (PM), and the others arose from empirical relationships (e.g. Thornthwaite method³⁵, TH) that need less parameters. The previous studies show that aerodynamic factors often have impacts in spring and winter of northern China, but the overall estimation of PET (in both temporal evolution and spatial distribution) from two methods are very comparable^{34,36}. Similar conclusions can also be found in Vicente-Serrano et al.³¹ and Mavromatis³⁷. Therefore, we adopted the TH method to calculate PET and SPEI considering data availability and natural features of QTP.

In this study, SPEI-annual and SPEI-seasonal were computed by using the SPEI package in the R software³⁸. The SPEI-annual and SPEI-seasonal were calculated from accumulation of climatic water balance during a 12-month period from the month to the preceding 12 months and a 3-month period from the month to the preceding 3 months, respectively. Among them, we identified specific SPEI values to present annual and seasonal conditions, i.e. SPEI-annual (the SPEI-12 of December) and SPEI-seasonal (the SPEI-3 of May, August, November and the next February for SPEI-spring, SPEI-summer, SPEI-autumn and SPEI-winter, respectively), linking to an estimation of meteorological drought. The detailed calculation steps of SPEI can be found in Vicente-Serrano et al.³¹. Table 1 shows the tentative range of SPEI and drought grade classification criteria.

Sen's slope. When using Mann–Kendall trend test (MK-test) to detect a changing trend of time series, Sen's slope is usually employed to estimate the magnitude of the trend as follows³⁹:

$$f(t) = Mt + C \quad (1)$$

where $f(t)$ is the function of the linear trend, M is the slope and C is the constant of the equation.

The formula of the trend's magnitude estimation is:

$$Q = \text{median} \frac{X_i - X_j}{t_i - t_j} \quad (2)$$

where x_i and x_j are the data values at times t_i and t_j ($i > j$), respectively.

Mann–Kendall test. The MK-test has been widely used in detecting the significance of Sen's slope of meteorological factors. In this study, the null hypothesis (H_0) is the SPEI series (x_1, x_2, x_3, \dots), which is an independent and uniformly distributed random variable with n data points, the alternative hypothesis (H_1) is a bilateral test, for all $k, j \leq n$ and $k \neq j$, x_k and x_j are distributed differently. The test statistical variable S is computed as follows:

$$S = \sum_{k=1}^{n-1} \sum_{j=k+1}^n \text{Sgn}(x_j - x_k) \quad (3)$$

where $\text{Sgn}(x)$ represents the sign function, which is computed as follows:

$$\text{Sgn}(x_j - x_k) = \begin{cases} +1 & x_j - x_k > 0 \\ 0 & x_j - x_k = 0 \\ -1 & x_j - x_k < 0 \end{cases} \quad (4)$$

S is distributed normally with a mean value of zero, and the variance can be expressed as:

$$\text{Var} = n(n-1)(2n+5)/18 \quad (5)$$

if n exceeded 10, the standard test statistical variable Z is computed as follows:

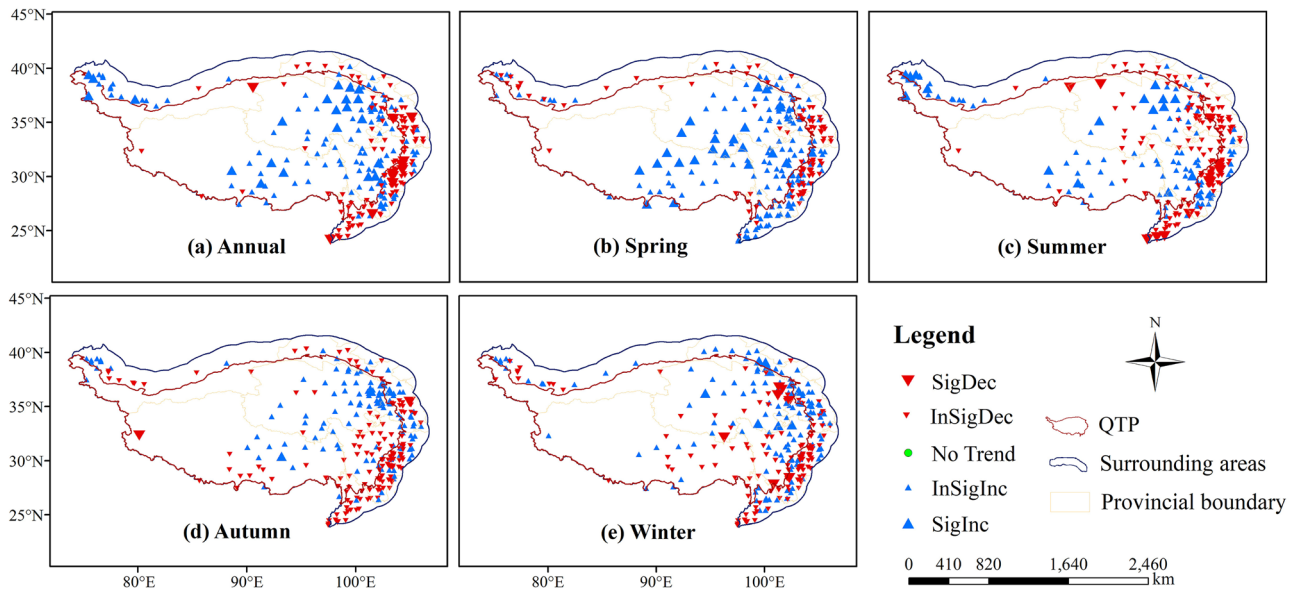


Figure 2. Annual and seasonal distributions of Z values at 274 meteorological stations: (a) Annual, (b) Spring, (c) Summer, (d) Autumn, (e) Winter. Blue, red triangle and green circle represent wetting, drying and no trends, respectively. The larger triangle indicates significant trends at 95% confidence level. The map was created using ArcMap 10.2, URL: <https://www.esrichina-bj.cn/softwareproduct/ArcGIS/>, the final figure was generated using Photoshop CC2018, URL: <https://onesoftwares.net/>.

$$Z = \begin{cases} \frac{S-1}{\sqrt{\text{Var}(S)}} & S > 0 \\ 0 & S = 0 \\ \frac{S+1}{\sqrt{\text{Var}(S)}} & S < 0 \end{cases} \quad (6)$$

In the bilateral test, if $|Z|$ is $\geq Z_{1-(p/2)}$ at the p significance level, the null hypothesis (H_0) is rejected, i.e., under the given confidence level of p , the time series show an upward ($Z > 0$) or downward trend ($Z < 0$). Specifically, $|Z| \geq 1.28, 1.96$ or 2.32 represent the trend of the time series passed the 90%, 95% or 99% confidence levels, respectively.

Rescaled range analysis. The Hurst index is used to predict the persistence of the time series. It can be computed by the method of rescaled range analysis (R/S)^{25,26}. The following are the calculation steps:

Firstly, divide the SPEI series (U) with length A into $[A/B]$ subsequences u_i ($i = 2, 3, \dots [A/B]$) with length B . The subsequences' extents are computed using the following formula:

$$R_u = \max Z_u - \min Z_u \quad (7)$$

where Z_u is the sequence cumulative bias of the subsequence of u_i .

Secondly, calculate Hurst's empirical formula ($R_N/S_N = \omega N^H$) for logarithmic processing as follows:

$$\log(R_N/S_N) = H \log N + \log \omega \quad (8)$$

where S_N is the standard bias of subsequence u_i , R_N/S_N is each subsequence's rescaled range, H is the Hurst index, and ω is a constant.

H ranges from 0 to 1 and can be categorized into three different intervals^{40,41}. If $0 < H < 0.5$, the trend of SPEI series in the future will reverse the current trend; if $0.5 < H < 1$, the SPEI series is likely to keep the current trend; and $H = 0.5$ indicates the SPEI series will exhibit a random trend in the future.

Results

Trend analysis of SPEI series. Figure 2 showed annual and seasonal distributions of temporal trends characterized by Z values at 274 meteorological stations. Annually, the SPEI-annual exhibited an increasing trend in more than 70% of the stations across the QTP (Fig. 2a), illustrating that most of the QTP were getting wetter with a mean rate of 0.0073/year (Table 2). While the surrounding areas were getting drier at the rate of -0.0033 /year with SPEI-annual decreasing in 64.8% stations. A total of 8 stations got drier significantly, mainly distributed in Gansu and Sichuan Provinces, but most stations in Yunnan Province showed slight drying trends.

Four seasons also experienced wetter trends in the QTP with the most significant trend of 0.0114/year in spring (Table 2, $p < 0.05$), when 90 stations showed an increasing trend and 21 of them were significant. While 15 drying stations were concentrated in a small part of Gansu and Sichuan Provinces (Fig. 2b). In summer, autumn and winter, more than 52% of the QTP stations got an increasing SPEI-seasonal, but approximately 65% of the surrounding stations showed decreasing SPEI-seasonal, indicating a drying trend contrary to the QTP (Fig. 2c-e).

Area	Annual	Spring	Summer	Autumn	Winter
QTP	0.0073	0.0114*	0.0023	0.0027	0.0030
Surrounding areas	-0.0033	0.0002	-0.0036	-0.0045	0.0020

Table 2. Annual and seasonal SPEI trends in the QTP and its surrounding areas. unit:/year. * indicates trends significant at $p < 0.05$.

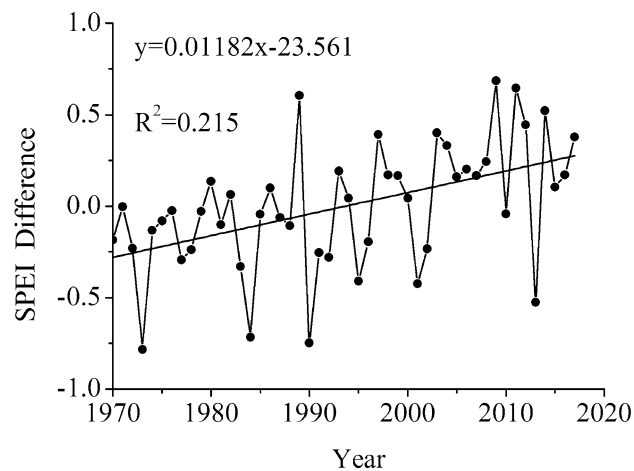


Figure 3. The difference of annual SPEI in the QTP and its surrounding areas.

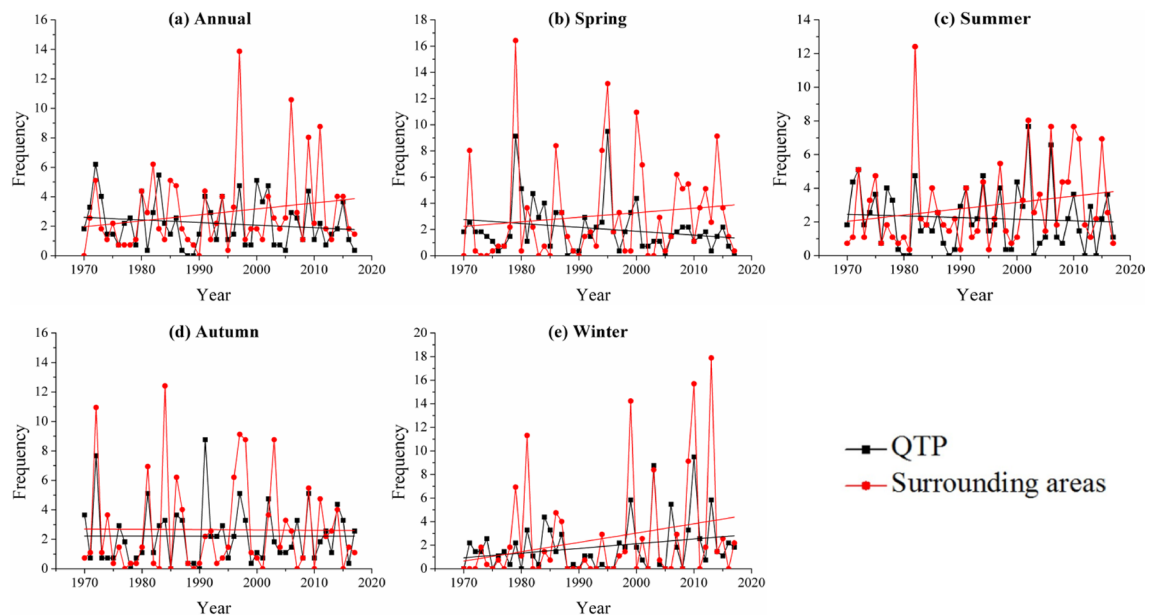


Figure 4. Annual and seasonal frequencies of severe drought: (a) Annual, (b) Spring, (c) Summer, (d) Autumn, (e) Winter in the QTP and its surrounding areas.

Apparently, the QTP was getting wetter particularly in spring during the past half century, while the surrounding areas (southeast part, in special) got significantly drier. The QTP had ever been drier than the surrounding areas in the early period but became wetter after 1994, and the difference kept growing up from then on (Fig. 3).

Temporal variation of severe drought. Figure 4 showed the annual and seasonal frequencies of severe drought events in the last half century. In general, the annual drought frequency of the QTP was decreasing while the surrounding areas exhibited an increasing trend. Before 1997, the differences of severe drought frequency between the QTP and its surrounding areas was not obvious (fluctuated in 0–6.2%), while in the last

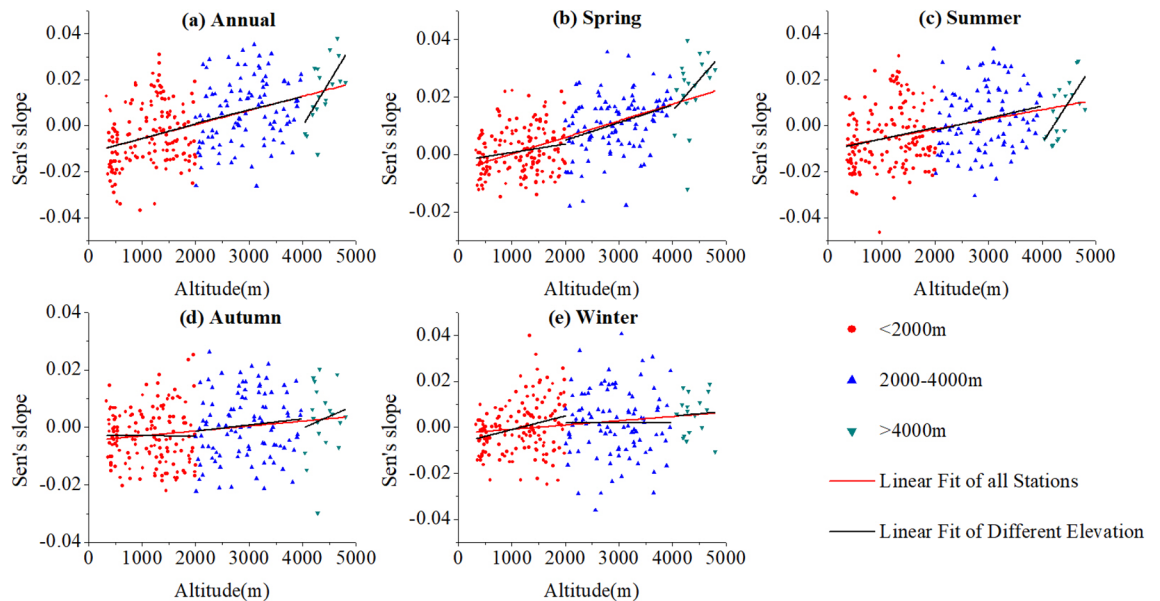


Figure 5. Relationships between SPEI trends and elevation: (a) Annual, (b) Spring, (c) Summer, (d) Autumn, (e) Winter in the QTP and its surrounding areas.

Time	Study region	Below 2000 m	2000–4,000 m	Above 4,000 m	Above 4,000 m vs. Study region (multiple)
Annual	0.00614*	0.00627*	0.00582*	0.03875*	6.3
Spring	0.00577*	0.00295*	0.00608*	0.02159*	3.7
Summer	0.00424*	0.00498*	0.00527*	0.03607*	8.5
Autumn	0.00171*	−0.000165	0.00212	0.00817	4.8
Winter	0.00184*	0.00593*	0.000119	0.00198	1.1

Table 3. The linear fit slopes of SPEI trends versus elevation on different altitudinal gradient. unit:/1,000 m. * indicates trends significant at $p < 0.05$.

two decades, large differences have appeared with severe drought frequency in the surrounding areas increasing from 1.1 to 13.9% but that in the QTP decreasing from 0.4 to 5.1% (Fig. 4a). This indicated that the surrounding areas were more prone to severe drought in recent years. For the four seasons, the frequency of severe drought has decreased in spring, summer, but increased in winter in the QTP (Fig. 4e). In surrounding areas, however, spring, summer and winter experienced higher severe drought frequency increasing, and autumn had no obvious variations.

Elevation dependence of SPEI trend. The relationship of Sen's slope of SPEI series from 274 meteorological stations versus the elevation were analyzed in Fig. 5 and Table 3. The significance level adopted here was $p < 0.05$. Apparently, stations in the high-elevation ranges showed more rapidly increasing trends in SPEI series than those at lower elevations. For the entire study region, SPEI trends at different time scales increased with elevation and all passed the significance test, indicating a wetter trend in higher elevation. Specifically, it was positively correlated with elevation below 2000 m and passed the significance test except for autumn. Trends at elevation between 2000 m and 4,000 m were similar to that below 2000 m, and the annual, spring and summer passed the significance test. The most rapidly increasing trend occurred above 4,000 m and passed the significance test except for autumn and winter. Additionally, change magnitudes of SPEI trends with increasing elevation above 4,000 m were most robust in annual and summer (Fig. 5a–c), which were about 6.3 and 8.5 times that of the entire study region, respectively.

In order to further explore the reasons, we analyzed the trends of three meteorological factors (temperature, precipitation and PET) that were used to compute SPEI. On the annual basis, for the elevation range above 4,000 m, the trends of temperature (T) and PET were negative but that of precipitation (P) was significantly positively correlated with elevation (Table 4), making a strong positive correlation between SPEI trend and elevation. For the other two elevation ranges (2000–4,000 m and below 2000 m), all trends of the three meteorological parameters were positively correlated with elevation, resulting in a weakly positive trend between of SPEI trend and elevation.

At the seasonal scale, similar to that in annual, faster wetting trends were detected in spring and summer for the elevation above 4,000 m. In autumn, although T and PET trends were negative and P trend was positive with

Seasons	Elevation	Correlation coefficient between the elevation and trends of meteorological factors		
		T	P	PET
Annual	<2000	0.386*	0.336*	0.046
	2000–4,000	0.123	0.217*	0.002
	>4,000	-0.106	0.651*	-0.126
Spring	<2000	0.192*	0.139	-0.047
	2000–4,000	-0.069	0.218*	-0.110
	>4,000	-0.036	0.246	-0.132
Summer	<2000	0.412*	0.350*	0.214*
	2000–4,000	0.159	0.161	0.021
	>4,000	-0.096	0.693*	-0.339
Autumn	<2000	0.349*	-0.054	0.047
	2000–4,000	0.168	0.136	0.047
	>4,000	-0.012	0.064	-0.018
Winter	<2000	0.482*	0.118	0.014
	2000–4,000	0.150	-0.087	0.132
	>4,000	-0.206	-0.097	0.032

Table 4. Correlation coefficients of seasonal trends with elevation for T, P and PET in 1970–2017. *indicates significant at $p < 0.05$.

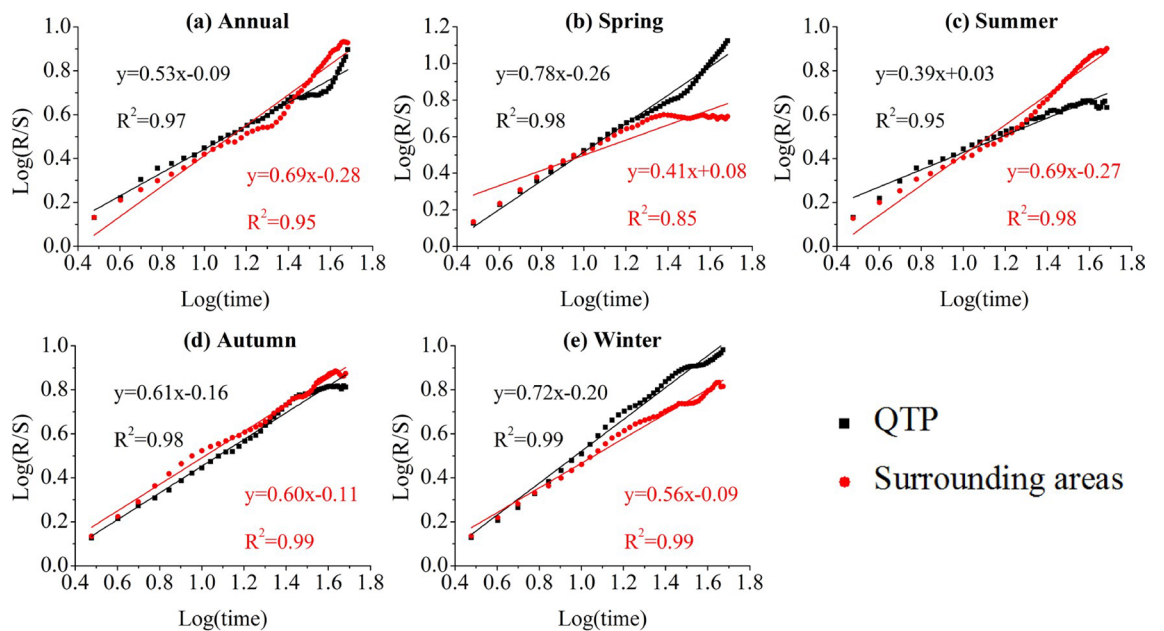


Figure 6. The rescaled range analysis of annual and seasonal SPEI series: (a) Annual, (b) Spring, (c) Summer, (d) Autumn, (e) Winter in the QTP and its surrounding areas.

elevation, the correlation coefficients were smaller, resulting in unobvious wetting trends with elevation. The opposite changes of P and PET trends with elevation from other seasons led to the stable SPEI trend in winter. In general, the negative changes of T and PET trends and the positive change of P trend may contribute to the rapid wetter condition above 4,000 m. This could be better confirmed in annual, spring and summer, when the phenomenons were more obvious.

Future persistence of drought. According to the variation of SPEI in the QTP and its surrounding areas over the last half century, R/S analysis was performed to evaluate the long-term correlation of time series⁴². Figure 6 showed the results of R/S analysis in different seasons. In general, the Hurst index of annual SPEI in the QTP and surrounding areas were 0.53 and 0.69, respectively, indicating the drought may maintain current trends, i.e. the QTP got wetter and surrounding areas got drier in the future (Fig. 6a). The persistence of SPEI series in the study region showed clear seasonal differences. In the QTP, only summer ($H=0.39$) exhibited small

trends that were predicted to be drier in the future but other three seasons would likely maintain current trends (H were 0.78, 0.61 and 0.72, respectively), indicating a wetter climate. In the surrounding areas, the existing drying trend would continue in summer ($H=0.69$) and autumn ($H=0.60$), winter ($H=0.56$) would keep the current wetter trend, and spring ($H=0.41$) would reverse the current trend to drier climate. Relevant stakeholders should therefore pay attention to prevent the potential damage of drought events in summer.

Discussion

Rapid wetting trends at high-elevation regions. Elevation is of great importance in analyzing the climate spatial changes in mountainous regions, particularly in the QTP. This study explored the elevation dependence of drought as well as its possible causes in the QTP and the surrounding areas from 1970 to 2017. We showed that wetter trends were positively correlated with elevation ($p < 0.05$), with the change trend above 4,000 m being 6.3 times higher than below, and the most significant difference was as high as 8.5 times in summer. In terms of meteorological parameters, negative changes of temperature and PET trends and positive change of precipitation trend were detected above 4,000 m, particularly in annual, spring and summer. All of them have caused the rapid wetter condition at highland regions.

Together with global warming that glaciers in the QTP rapidly shrinks⁴³, more streamflow was yielded in the region²⁵. We concluded that the surrounding areas easily suffered from meteorological drought. However, this might be compensated by more streamflow at the low altitudes due to the upstream glacier melting. Glaciers are a uniquely drought resilient source of water, which may pose an important but underappreciated role in protecting downstream populations from the worst effects of droughts⁴⁴. Glacial meltwater is also a source recharging river headwaters and downstream runoff in the QTP^{45,46}. Previous studies showed that the runoff from headwater area of the QTP would be rising in future decades^{47,48}, while the downstream precipitation was decreasing in the surrounding areas. This leads to the greater contribution and influence of runoff changes in the upstream on the downstream; for example, 70% runoff of Nujiang River in Yunnan Province comes from the upper reaches⁴⁹. Affected by upstream water inflow, the scope and level of hydrological drought in downstream areas are weaker than those of meteorological drought^{50,51}. Investigating the contribution of glaciers melting to the lower reaches of rivers is therefore necessary in the future, which can provide solid assistance for downstream drought adaptation.

It is worth noting that, although the QTP has become wetter, severe drought frequency in winter has increased, indicating that winter was more prone to severe droughts. This could not only reduce soil moisture, affect the growth of overwintering crops and the emergence of spring-sown crops but also endanger human and livestock drinking water. More violent fluctuations of severe drought events in the surrounding areas could be an omen of flash drought, which may bring devastating impacts on crop yields and water supply and further trouble the people as for less effective response^{52–54}. The risk of flash drought in this region in the future thus deserved more attention of local authorities.

Consistency of different drought indices. The selection of duration, indices and purposes, as well as the quality of data sources would all affect the results. Previously, many indices were used to identify the drought trends, frequency and severity in the QTP, such as the Palmer Drought Severity Index (PDSI)⁵⁵, the Standardized Precipitation Index (SPI)⁵⁶ and Temperature Vegetation Dryness Index (TVDI)⁵⁷. Among them, PDSI may incorporate many climatic parameters (e.g. prior precipitation, moisture supply, runoff, evaporation demand) but is only applicable for mid- and long-term droughts due to the strong lagged autocorrelation^{58,59}. SPI, on the other hand, only involves precipitation and shows high uncertainty in describing the drought in summer and winter; whereas SPEI simultaneously considers precipitation and evapotranspiration, and thus can accurately capture the effects of drought under the background of global warming.

To validate the findings of this study, we further compared with some previous achievements using other drought indices and data sources in the QTP (Table 5). Our results confirmed the wetting trend in the QTP with the most significant level in spring reported by previous studies^{8,16,17,60}. Meanwhile, the use of different methods to calculate PET of the SPEI generated similar results, all indicating the eastern QTP becoming drier^{14,17,32}. However, this spatial pattern showed conflict with Yu et al.⁶¹ and Wang et al.¹⁸ They reported a wetting trend in the eastern QTP and a significant drying trend in the north in spring and autumn. A number of stations, length of study period and slightly different regions may contribute to the differences, demonstrating the importance of adequate high-quality data and careful selection of study area when investigated the spatial-temporal changes of drought in the QTP.

Conclusions

In this study, we analyzed the SPEI from 274 meteorological stations in the QTP and its surrounding areas during 1970–2017 and draw the following conclusions. Firstly, drought characteristics between the QTP and its surrounding areas have great differences: a wetting trend existed in the QTP with spring getting wet mostly at the rate of 0.0114/year, while the surrounding areas showed a drying trend, especially in Yunnan Province; the difference between SPEI in the QTP and its surrounding areas has increased from -0.19 in 1970 to 0.38 in 2017. Secondly, although a wetter climate in the QTP, we found the severe drought frequency in winter has substantially increased, which indicated winter was more prone to severe drought. Thirdly, SPEI trend exhibited an elevation dependence, which generally increased with elevation, the change trend along elevation above 4,000 m was about 6.3 times higher than ones below 4,000 m. This was mainly caused by the decreasing temperature and PET trends and increasing precipitation trend. Lastly, in the future, the QTP and its surrounding areas would continue to be wetter and drier, respectively, and occurrence of future drought is most likely to increase in summer. The findings provided the basis for related researches, improved our understanding of the responses of dry and wet conditions to climate change across the QTP, and provided early warning for regional drought and

Region and station number	Period	Drought index	Main conclusions	References
QTP, 274	1970–2017	SPEI-TH	Got wetter mostly in spring Surrounding areas and several Eastern QTP stations became drier Increased severe drought in winter Drier summer in the future	This study
QTP, 83	1979–2011	P/PET	Significantly wetting in the northwestern QTP Insignificant drying in half of the eastern QTP	Gao et al. ⁸
QTP, 74	1980–2014	SPEI-PM	Wetting in general Droughts detected in 75% stations Several northeastern and southern stations got drier	Liang et al. ¹⁴
China, 541	1994–2013	SPI, SPEI-PM	Drought relieved in the QTP Significantly wetting in spring Weakly wetting in summer and autumn Insignificant drying in winter	Wang et al. ¹⁶
China, 633	1961–2012	SPI, SPEI-PM	Wetting from the central to the northeastern part of the QTP Significant wetting in the middle/eastern QTP in April and May Drying trend of north QTP in February	Wang et al. ¹⁷
Mainland of China except for the arid region	1960–2012	A 3-dimensional clustering method based on the SPI3, RDI3 and SPEI3	Significant wetting trend over the QTP	Xu et al. ³²
China, grid (0.5° × 0.5° resolution)	1961–2009	scPDSI	Significant wetting in the southern QTP Spring and autumn got drier in the northern QTP	Wang et al. ¹⁸
China, 509	1951–2010	SPEI-TH	Wetting trend in the eastern QTP with the drought frequency decreased	Yu et al. ⁶¹

Table 5. Comparisons with previous conclusions using different drought indices.

references for drought disaster prevention and mitigation. However, the underlying mechanism of the drought pattern needs to be further explored.

Data availability

The meteorological datasets used in this study are available in the Data Center for Resources and Environmental Sciences, Chinese Academy of Sciences (<https://www.resdc.cn/>).

Received: 7 February 2020; Accepted: 6 August 2020

Published online: 31 August 2020

References

1. Yao, N., Li, Y., Lei, T. & Peng, L. Drought evolution, severity and trends in mainland China over 1961–2013. *Sci. Total. Environ.* **616–617**, 73–89. <https://doi.org/10.1016/j.scitotenv.2017.10.327> (2018).
2. Yusa, A. *et al.* Climate change, drought and human health in Canada. *Int. J. Environ. Res. Public Health.* **12**, 8359–8412. <https://doi.org/10.3390/ijerph120708359> (2015).
3. Liu, L., Niu, Q., Heng, J., Li, H. & Xu, Z. Transition characteristics of the dry-wet regime and vegetation dynamic responses over the Yarlung Zangbo River Basin, Southeast Qinghai-Tibet Plateau. *Remote Sens.* <https://doi.org/10.3390/rs11101254> (2019).
4. Dai, A. Drought under global warming: A review. *Wiley. Interdiscip. Rev. Clim. Chang.* **2**, 45–65. <https://doi.org/10.1002/wcc.81> (2011).
5. Chen, H. & Sun, J. Changes in drought characteristics over china using the standardized precipitation evapotranspiration index. *J. Clim.* **28**, 5430–5447. <https://doi.org/10.1175/jcli-d-14-00707.1> (2015).
6. Wang, B., Bao, Q., Hoskins, B., Wu, G. & Liu, Y. Tibetan Plateau warming and precipitation changes in East Asia. *Geophys. Res. Lett.* **35**, L14702. <https://doi.org/10.1029/2008GL034330> (2008).
7. Yang, K. *et al.* Recent climate changes over the Tibetan Plateau and their impacts on energy and water cycle: A review. *Glob. Planet. Change.* **112**, 79–91. <https://doi.org/10.1016/j.gloplacha.2013.12.001> (2014).
8. Gao, Y., Li, X., Ruby Leung, L., Chen, D. & Xu, J. Aridity changes in the Tibetan Plateau in a warming climate. *Environ. Res. Lett.* **10**, 034013. <https://doi.org/10.1088/1748-9326/10/3/034013> (2015).
9. Li, L., Yang, S., Wang, Z., Zhu, X. & Tang, H. Evidence of warming and wetting climate over the Qinghai-Tibet plateau. *Arct. Antarct. Alp. Res.* **42**, 449–457. <https://doi.org/10.1657/1938-4246-42.4.449> (2010).
10. Fan, K. *et al.* Variation, causes and future estimation of surface soil moisture on the Tibetan Plateau. *Acta. Geogr. Sin.* **74**, 520–533. <https://doi.org/10.11821/dlxb201903009> (2019).
11. Yang, K. *et al.* Response of hydrological cycle to recent climate changes in the Tibetan Plateau. *Clim. Change.* **109**, 517–534. <https://doi.org/10.1007/s10584-011-0099-4> (2011).
12. Yin, Y., Wu, S., Zhao, D., Zheng, D. & Pan, T. Impact of climate change on actual evapotranspiration on the Tibetan Plateau during 1981–2010. *Acta. Geogr. Sin.* **67**, 1471–1481. <https://doi.org/10.11821/xb201211004> (2012).
13. Liu, X. *et al.* Regionalization and spatiotemporal variation of drought in china based on standardized precipitation evapotranspiration index (1961–2013). *Adv. Meteorol.* **1–18**, 2015. <https://doi.org/10.1155/2015/950262> (2015).
14. Liang, J. *et al.* Drought evolution characteristics on the Tibetan Plateau based on daily standardized precipitation evapotranspiration index. *J. Glaciol. Geocryol.* **40**, 1100–1109. <https://doi.org/10.7522/j.issn.1000-0240.2018.0412> (2018).
15. Yang, X. L. *et al.* Drought assessment and trends analysis from 20th century to 21st century over China. *Proc. IAHS.* **371**, 89–94. <https://doi.org/10.5194/piahs-371-89-2015> (2015).
16. Wang, H., Chen, Y., Pan, Y., Chen, Z. & Ren, Z. Assessment of candidate distributions for SPI/SPEI and sensitivity of drought to climatic variables in China. *Int. J. Climatol.* **39**, 4392–4412. <https://doi.org/10.1002/joc.6081> (2019).
17. Wang, W., Zhu, Y., Xu, R. & Liu, J. Drought severity change in China during 1961–2012 indicated by SPI and SPEI. *Nat. Hazards.* **75**, 2437–2451. <https://doi.org/10.1007/s11069-014-1436-5> (2014).

18. Wang, Z. *et al.* Does drought in China show a significant decreasing trend from 1961 to 2009?. *Sci. Total Environ.* **579**, 314–324. <https://doi.org/10.1016/j.scitotenv.2016.11.098> (2016).
19. Messerli, B. & Ives, J. D. *Mountains of the World: A Global Priority*. Parthenon, 510pp.
20. Rangwala, I. & Miller, J. R. Climate change in mountains: A review of elevation-dependent warming and its possible causes. *Clim. Change.* **114**, 527–547. <https://doi.org/10.1007/s10584-012-0419-3> (2012).
21. Pepin, N. *et al.* Elevation-dependent warming in mountain regions of the world. *Nat. Clim. Change.* **5**, 424–430. <https://doi.org/10.1038/NCLIMATE2563> (2015).
22. Barry, R. G. Recent advances in mountain climate research. *Theor. Appl. Climatol.* **110**, 549–553. <https://doi.org/10.1007/s00704-012-0695-x> (2012).
23. Xu, Y., Ramanathan, V. & Washington, W. M. Observed high-altitude warming and snow cover retreat over Tibet and the Himalayas enhanced by black carbon aerosols. *Atmos. Chem. Phys.* **16**, 1303–1315. <https://doi.org/10.5194/acp-16-1303-2016> (2016).
24. Ding, M., Li, L., Zhang, Y., Liu, L. & Wang, Z. Temperature change and its elevation dependency on the Tibetan plateau and its vicinity from 1971 to 2012. *Resour. Sci.* **36**, 1509–1518 (2014).
25. Zhang, X., Wang, L. & Chen, D. How does temporal trend of reference evapotranspiration over the Tibetan Plateau change with elevation?. *Int. J. Climatol.* **39**, 2295–2305. <https://doi.org/10.1002/joc.5951> (2019).
26. Li, X., Wang, L., Guo, X. & Chen, D. Does summer precipitation trend over and around the Tibetan Plateau depend on elevation?. *Int. J. Climatol.* **37**, 1278–1284. <https://doi.org/10.1002/joc.4978> (2017).
27. Yao, T., Lu, H., Feng, W. & Yu, Q. Evaporation abrupt changes in the Qinghai–Tibet Plateau during the last half-century. *Sci. Rep.* **9**, 20181. <https://doi.org/10.1038/s41598-019-56464-1> (2019).
28. Tian, P., Lu, H. & Xue, Y. Characterization of temperature difference between the neighbouring days in China and its potential driving factors. *Int. J. Climatol.* **39**, 4659–4668. <https://doi.org/10.1002/joc.6093> (2019).
29. Ding, J., Cuo, L., Zhang, Y. & Zhu, F. Monthly and annual temperature extremes and their changes on the Tibetan Plateau and its surroundings during 1963–2015. *Sci. Rep.* **8**, 11860. <https://doi.org/10.1038/s41598-018-30320-0> (2018).
30. Yao, T., Lu, H., Yu, Q. & Feng, W. Potential evapotranspiration characteristic and its abrupt change across the Qinghai–Tibetan Plateau and its surrounding areas in the last 50 years. *Adv. Earth. Sci.* **35**, 534–546. <https://doi.org/10.11867/j.issn.1001-8166.2020.031> (2020).
31. Vicente-Serrano, S. M., Beguería, S. & López-Moreno, J. I. A multiscalar drought index sensitive to global warming: The standardized precipitation evapotranspiration index. *J. Clim.* **23**, 1696–1718. <https://doi.org/10.1175/2009jcli2909.1> (2010).
32. Xu, K. *et al.* Spatio-temporal variation of drought in China during 1961–2012: A climatic perspective. *J. Hydrol.* **526**, 253–264. <https://doi.org/10.1016/j.jhydrol.2014.09.047> (2015).
33. Li, W., Yi, X., Hou, M., Chen, H. & Chen, Z. Standardized precipitation evapotranspiration index shows drought trends in China. *Chin. J. Eco-Agric.* **20**, 643–649. <https://doi.org/10.3724/SPJ.1011.2012.00643> (2012).
34. Beguería, S., Vicente-Serrano, S. M., Reig, F. & Latorre, B. Standardized precipitation evapotranspiration index (SPEI) revisited: Parameter fitting, evapotranspiration models, tools, datasets and drought monitoring. *Int. J. Climatol.* **34**, 3001–3023. <https://doi.org/10.1002/joc.3887> (2014).
35. Thornthwaite, C. W. An approach toward a rational classification of climate. *Geogr. Rev.* **38**, 55–94. <https://doi.org/10.2307/210739> (1948).
36. Xu, C. Y. & Singh, V. P. Evaluation and generalization of temperature-based methods for calculating evaporation. *Hydrol. Process.* **15**, 305–319. <https://doi.org/10.1002/hyp.119> (2001).
37. Mavromatis, T. Drought index evaluation for assessing future wheat production in Greece. *Int. J. Climatol.* **27**, 911–924. <https://doi.org/10.1002/joc.1444> (2007).
38. Beguería, S. & Vicente-Serrano, S. M. SPEI: calculation of the standardised precipitation–evapotranspiration index. <https://CRAN.R-project.org/package=SPEI> (2017).
39. Sen, P. K. Estimates of the regression coefficient based on Kendall's Tau. *J. Am. Assoc.* **63**, 1379–1389. <https://doi.org/10.1080/01621459.1968.10480934> (1968).
40. Hurst, H. E. Long-Term storage capacity of reservoirs. *Trans. Am. Soc. Civ. Eng.* **116**, 770–808 (1951).
41. Mandelbr, B. & Wallis, J. R. Robustness of rescaled range R/S in measurement of noncyclic long run statistical dependence. *Water Resour. Res.* **5**, 967–988. <https://doi.org/10.1029/WR005i005p0967> (1969).
42. Zhao, X., Li, Z. & Zhu, Q. Change of precipitation characteristics in the water–wind erosion crisscross region on the Loess Plateau, China, from 1958 to 2015. *Sci. Rep.* **7**, 8048. <https://doi.org/10.1038/s41598-017-08600-y> (2017).
43. Yao, T. *et al.* Different glacier status with atmospheric circulations in Tibetan Plateau and surroundings. *Nat. Clim. Chang.* **2**, 663–667. <https://doi.org/10.1038/NCLIMATE1580> (2012).
44. Pritchard, H. D. Asia's shrinking glaciers protect large populations from drought stress. *Nature* **569**, 649–654. <https://doi.org/10.1038/s41586-019-1240-1> (2019).
45. Tang, Q. *et al.* Streamflow change on the Qinghai–Tibet Plateau and its impacts. *Chin. Sci. Bull.* **64**, 2807–2821. <https://doi.org/10.1360/TB-2019-0141> (2019).
46. Tian, P., Lu, H., Feng, W., Guan, Y. & Xue, Y. Large decrease in streamflow and sediment load of Qinghai–Tibetan Plateau driven by future climate change: A case study in Lhasa River Basin. *CATENA* **187**, 104340. <https://doi.org/10.1016/j.catena.2019.104340> (2020).
47. Luo, Y. *et al.* Contrasting streamflow regimes induced by melting glaciers across the Tien Shan–Pamir–North Karakoram. *Sci. Rep.* **8**, 16470. <https://doi.org/10.1038/s41598-018-34829-2> (2018).
48. Lutz, A. F., Immerzeel, W. W., Shrestha, A. B. & Bierkens, M. F. P. Consistent increase in High Asia's runoff due to increasing glacier melt and precipitation. *Nat. Clim. Chang.* **4**, 587–592. <https://doi.org/10.1038/NCLIMATE2237> (2014).
49. Li, Y., Wang, Z., Zhang, Y., Li, X. & Huang, W. Drought variability at various timescales over Yunnan Province, China: 1961–2015. *Theor. Appl. Climatol.* **138**, 743–757. <https://doi.org/10.1007/s00704-019-02859-z> (2019).
50. Wu, Z. *et al.* Exploring spatiotemporal relationships among meteorological, agricultural, and hydrological droughts in Southwest China. *Stoch. Environ. Res. Risk Assess.* **30**, 1033–1044. <https://doi.org/10.1007/s00477-015-1080-y> (2016).
51. Rong, Y., Gong, L. & Lu, S. Analysis on characteristics and causes of persistent meteorological and hydrological drought in Yunnan from 2009 to 2014. *Water Resour. Prot.* **34**, 22–29. <https://doi.org/10.3880/j.issn.1004-6933.2018.03.04> (2018).
52. Ford, T. W., McRoberts, D. B., Quiring, S. M. & Hall, R. E. On the utility of in situ soil moisture observations for flash drought early warning in Oklahoma, USA. *Geophys. Res. Lett.* **42**, 9790–9798. <https://doi.org/10.1002/2015GL066600> (2015).
53. Otkin, J. A. *et al.* Assessing the evolution of soil moisture and vegetation conditions during the 2012 United States flash drought. *Agric. Forest. Meteorol.* **218–219**, 230–242. <https://doi.org/10.1016/j.agrformet.2015.12.065> (2016).
54. Wang, L., Yuan, X., Xie, Z., Wu, P. & Li, Y. Increasing flash droughts over China during the recent global warming hiatus. *Sci. Rep.* **6**, 30571. <https://doi.org/10.1038/srep30571> (2016).
55. Palmer. Meteorological drought. *Weather Bureau Research Paper.* **45** (1965).
56. Patel, N. R. & Chopra, P. Analyzing spatial patterns of meteorological drought using standardized precipitation index. *Theor. Appl. Climatol.* **14**, 329–336. <https://doi.org/10.1002/met.33> (2007).
57. Sandholt, I., Rasmussen, K. & Andersen, J. A simple interpretation of the surface temperature/vegetation index space for assessment of surface moisture status. *Remote Sens. Environ.* **79**, 213–224. [https://doi.org/10.1016/S0034-4257\(01\)00274-7](https://doi.org/10.1016/S0034-4257(01)00274-7) (2002).

58. Zhai, J. *et al.* Spatial variation and trends in PDSI and SPI indices and their relation to streamflow in 10 large regions of China. *J. Clim.* **23**, 649–663. <https://doi.org/10.1175/2009JCLI2968.1> (2010).
59. Zhao, H. *et al.* Timescale differences between SC-PDSI and SPEI for drought monitoring in China. *Phys. Chem. Earth.* **102**, 48–58. <https://doi.org/10.1016/j.pce.2015.10.022> (2017).
60. Liu, L. *et al.* Changes in aridity and its driving factors in China during 1961–2016. *Int. J. Climatol.* **39**, 50–60. <https://doi.org/10.1002/joc.5781> (2019).
61. Yu, M., Li, Q., Hayes, M. J., Svoboda, M. D. & Heim, R. R. Are droughts becoming more frequent or severe in China based on the standardized precipitation evapotranspiration Index: 1951–2010?. *Int. J. Climatol.* **34**, 545–558. <https://doi.org/10.1002/joc.3701> (2014).

Acknowledgements

This research was supported by the Strategic Priority Research Program of the Chinese Academy of Sciences [XDA20040301] and the Second Tibetan Plateau Scientific Expedition and Research Program (STEP) [2019QZKK1003].

Author contributions

H.L. conceived the idea. W.F. designed the study and analyzed the data. W.F. and T.Y. contributed to the interpretation and manuscript writing. H.L. revised the paper. W.F., H.L., T.Y., and Q.Y. reviewed the manuscript.

Competing interests

The authors declare no competing interests.

Additional information

Correspondence and requests for materials should be addressed to H.L.

Reprints and permissions information is available at www.nature.com/reprints.

Publisher's note Springer Nature remains neutral with regard to jurisdictional claims in published maps and institutional affiliations.



Open Access This article is licensed under a Creative Commons Attribution 4.0 International License, which permits use, sharing, adaptation, distribution and reproduction in any medium or format, as long as you give appropriate credit to the original author(s) and the source, provide a link to the Creative Commons licence, and indicate if changes were made. The images or other third party material in this article are included in the article's Creative Commons licence, unless indicated otherwise in a credit line to the material. If material is not included in the article's Creative Commons licence and your intended use is not permitted by statutory regulation or exceeds the permitted use, you will need to obtain permission directly from the copyright holder. To view a copy of this licence, visit <http://creativecommons.org/licenses/by/4.0/>.

© The Author(s) 2020